Contents lists available at ScienceDirect

Journal of King Saud University – Science

journal homepage: www.sciencedirect.com

Original article

Effect of laser shock peening on the hardness of AL-7075 alloy

Ayman M. Mostafa [a,b,*], Mohamed F. Hameed [c,d], Salah S. Obayya [c,d]

[a] Spectroscopy Department, Physics Division, National Research Centre, Dokki, Cairo, Egypt
[b] Laser Technology Unit, Center of Excellence for Advanced Sciences (CEAS), National Research Centre, Dokki, Cairo, Egypt
[c] Centre for Photonics and Smart Materials (CPSM), Zewail City of Science and Technology, Giza, Egypt
[d] Faculty of Engineering, Mansoura University, Mansoura, Egypt

ABSTRACT

Laser shock peening (LSP) is a surface treatment process for increasing the strength and reliability of metal components. Traditionally applied to composite structures of automotive and medical applications, the LSP technology also shows great potential for aircraft parts to improve the fatigue resistance of highly stressed critical aircraft turbine engine components, complex forming of wing surfaces, steam turbines, etc. The present study investigates the effect of laser peening without coating on the hardness of an aluminium alloy. The Vickers micro-hardness test is used to study the hardness of the Al alloy with different wavelengths and laser intensities. It is found that the metal hardness can be significantly increased to more than 80% by increasing the laser intensity and the number of laser shots irradiated per unit area.

1. Introduction

In the previous four decades, aluminium alloys have been widely used in the aircraft, automotive, marine and construction industries, due to their low cost, good weight/strength ratio and high corrosion resistance (Vargel, 2004; Panagopoulos et al., 2009; Bajat et al., 2010). In addition, elongation to failure as high as about 2000% can be obtained (Smolej et al., 2012) by using aluminium alloys with the addition of Sc and Zr superplastic properties. The applications of light metal alloys like aluminium in industries have been promoted continuously to meet the requirements of lightening under the pressure of energy shortage and the rise of fuel prices (Trueba and Trasatti, 2010; O'Regan, 1991). However, the surface hardness and wear resistance of aluminium alloys are usually poor, which, to a large extent, limits their service lifetime. Hence, the surface strengthening processing technology of light metal alloys has become more and more important (O'Regan, 1991; Ezuber et al., 2008; Yue et al., 2006).

In order to reduce the surface roughness and deepen the compressive residual stresses distribution, many new peening technologies such as laser peening (Montross et al., 2002), cavitation shotless peening (Odhiambo and Soyama, 2003), ultrasonic peening (Brus, 1984) and microshot peening (Oguri, 2011; Harada et al., 2007) were developed. Among these peening technologies, laser shock peening (LSP) technique, as an alternative surface promising technology, was demonstrated and explored for the first time at sixties by Fairand and Clauer (Fairand and Clauer, 1976) and co-workers (Graham and Yang, 1975; Fairand et al., 1974, 1972; White, 1963). Initially, LSP was developed for the aeronautic industry for the improvement of the resistance to fatigue cracking for some applications such as aircraft engine components, airframes, and other engineering applications. This is because the LSP was considered as one of the most promising surface enhancement techniques in terms of its ability to induce surface compressive residual stress, surface hardness and microstructure modifications (Brus, 1984). In addition, the LSP has been applied successfully to improve the damage tolerance of several critical compressor blades leading edges. For instance, LSP can be used to increase the resistance of a metal to crack initiation, extend the fatigue life, and enhance the fatigue strength (Ding and Ye, 2006a; Kazakevich et al., 2006; Yuji Sano et al., 2006). This treatment is imparted by the shockwaves resulting from the expansion of high-pressure plasma generated by an intense pulsed laser (Ding and Ye, 2006a; Kazakevich et al., 2006; Yuji Sano et al., 2006).

The basic principle behind LSP can be explained as follows. A high power pulsed laser is focused onto the target material surface

* Corresponding author at: Spectroscopy Department, Physics Division, National Research Centre, Dokki, Cairo, Egypt.
E-mail addresses: aymanmdarwish@gmail.com (A.M. Mostafa), mfarahat@zewailcity.edu.eg (M.F. Hameed), sobayya@zewailcity.edu.eg (S.S. Obayya).

Production and hosting by Elsevier

by using a lens. Then when the laser energy exceeds the ablation threshold value for the material, chemical bonds are broken and the material is fractured into energetic fragments, typically a mixture of electrons, neutral atoms, molecules, and ions. Then a shockwave is induced in the target metal by generating plasma on its surface and the target surface layer evaporates instantaneously. The vapor continuously absorbs the laser energy for the entire pulse duration. This process converts the vapor to high temperature plasma. The plasma is an outcome of the gas phase, which absorbs the energy directly from the laser radiation and from the reflection of the material surface.

The plasma causes a shock wave by its expansion as laser intensities exceeding 10^{10}W/cm^2, a shockwave is generated due to the ignition and explosive expansion of the plasma. The plastic deformation caused by the shockwave while propagating through the metal results in the hardening of the metal surface and the generation of a surface with residual compressive stresses (Hu and Yao, 2008).

Shock waves in the solids, a strong sudden discontinuity of the pressure and of the associated parameters (Zeldovich and Raizer, 1967), belong to our environment since the dawn of times. The high power pulsed lasers came to be added in the panoply of shock generators, making it possible to induce pressures much higher than the precedents, but in extremely shorter times (Cauble et al., 1993). The shock wave is a result of ablation of material layers due to intensive absorption of laser radiation. The confined ablation consists in covering the target by a transparent medium to the laser radiation (water, glass, air), slowing down the plasma expansion in the surrounding atmosphere and causes up to ten times higher pressure on the material surface (Barmina et al., 2010; Fabbro et al., 1990). Furthermore, the hardness could be increased more times compared to the base alloy hardness, whereby the increase of hardness is due to dislocations generated in the shock affected region. It is assumed that residual stresses and work hardening are the reason of corrosion improvement, mainly by interface-like effects around the inclusions (Peyre et al., 2000).

The propagation of shock waves inside material through a schematic space/time diagram is presented in Fig. 1. Shock wave propagates through the target according to properties depending on the material characteristics and geometry. In a short distance, the shock front could be seen as a plane at the central area, and the material is compressed mainly by the longitudinal shock pressure. When reaching the sample back face, this incident shock wave is reflected into a release wave propagating backwards. This release wave is crossing the incident unloading wave coming from the front face and initiated by the end of the loading (back to the initial state). This crossing of two release waves can lead to a local high tensile stress area which could damage the material and lead, depending on the laser parameters, to the well-known spallation phenomenon (Romain et al., 2013).

In practice two different LSP processes are known (Ding and Ye, 2006b). The first one uses protective coating or absorbent layer in order to prevent the material surface from melting or being damaged. The coating is usually formed with a black paint or Al foil prior to laser irradiation, and the remaining coating is removed after the treatment. The second LSP process is called laser peening without coating (LPwC) which was discovered in 1995 (Besner et al., 2005). In general, both LSP processes require a unique high power density, high repetition laser, which enables plasma generation at the moment of the interaction of laser light and propagation of shock impact waves in the material (Trdan et al., 2010; Peyre et al., 1996). In this paper, the LPwC is used for increasing the metal hardness with increasing the number of laser shots irradiated per unit area and by increasing the laser intensity. Most of the recent researches have been focusing on studying the effects of the LSP processing parameters such as the laser energy (Rubio-González et al., 2011, 2004; Darwish et al., 2015), impact number (Zhou et al., 2012; Zhang et al., 2010; Darwish et al., 2016), sample geometry (Yang et al., 2001), laser spot size (Warren et al., 2008), surface integrity and fatigue life of alloys. However, few attentions have been paid to the effects of the LSP on the hardness properties.

Since the development of the LSP, a number of patents have been issued addressing its strong interest for increasing the hardness of Al alloy. A combination of high mechanical strength as well as good corrosion resistance has made Al based alloys a potential component in aerospace as well as automotive and shipping industries. Among them, Al-7075 has found widespread application due to good weldability and mechanical strength (Gomez-Rosas et al., 2010; Barcikowski et al., 2007; Mutombo and Toit, 2011). In 1996, Peyre et al. (1996) increased the hardness of 7075 Al alloys by 10%. This research (Peyre et al., 1996) had progressed well with several advantages in this field and had been evaluated the role of the LSP process on the cyclic properties of A356, AII2Si and 7075 aluminium alloys. In addition, Montross and Florea (2001) used the LSP to analyze the effect of the paint and foil coatings on the shockwave propagation into the 2011-T3 Al alloy. In this study (Montross and Florea, 2001), the hardness of the specimen is increased by 15%. Furthermore, Rodopoulos et al. (2003) made a comparative study between the LSP, and traditional treatments on the 2024-T351 Al Alloy. It was found that the LSP caused negligible strain hardening as in the other methods. Moreover, the multi treatments exhibited a far more superior fatigue improvement compared to the other methods. Then in 2004, Barcikowski et al. (2007) studied the reduction of fatigue crack growth by increasing the laser energy of 6061-T6 Al alloy to improve is mechanical property. Next in 2007, Masaki et al. (2007) firstly introduced the laser shock peening without coating (LPwC) to the degassing process which is useful for decreasing the casting defects in cast aluminium alloys and for improving the fatigue strength. In this regards, the specimen hardness was increased by 30%. Afterword, Ochi et al. (2010) developed a series of studies of LPwC on A7050-T7451 Al alloy to improve the fatigue strength and the hardness was increased by 10%. In 2012, Sathyajith and Kalainathan (Sathyajith and Kalainathan, 2012) successfully performed LSP on precipitation hardened aluminium alloy 6061-T6 with low energy (300 mJ,1064 nm) Nd:YAG laser using different laser energies which increased the hardness by 20%. Similarly, Vázquez et al. (2012) and Zhou et al. (2012) used the LSP technique to increase the hardness of the 7075-T651 Al alloy and 5A06 Al alloy by 25% and 20%, respectively. Then Trdan et al. (2012) studied the LSP effect at two laser energies of the AA6082-T651 Al alloy by
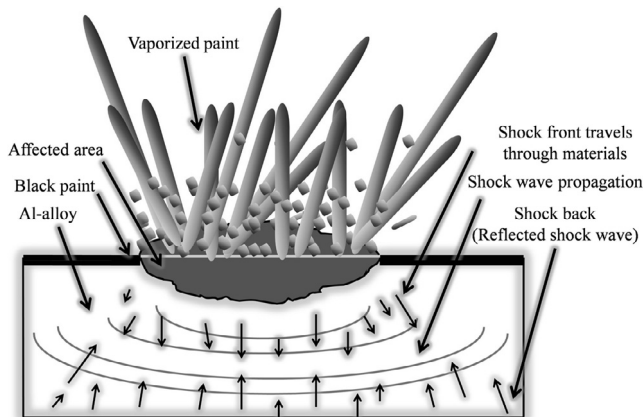

Fig. 1. schematic diagram of shock waves propagation through material.

using Vickers micro-hardness through depth variation in the near surface layer. It is evident from these results that the micro-hardness depth profile at both laser energies can be increased by the LPwC. Thus, the LPwC process can improve the mechanical properties of the alloy. In 2013, Sathyajith et al. (2013) used the LPwC to increase the hardness of the 6061-T6 Al alloy by 20%. This study showed that the LPwC can significantly improve surface compressive stress and micro-hardness with a little bit increasing in the surface roughness.

In the present work we successfully performed LPwC on the aluminium alloy Al-7075 type. The effect of the LPwC on the hardness of the alloy was investigated. It is found that the hardness of the alloy can be significantly increased by more than 80% by increasing the laser energy up to 0.9 J, number of pulses up to 300 pulses, and laser spot size in the range of few millimeters.

2. Material and methods

2.1. Materials

The Al 7075 alloy is widely used in aerospace and automotive manufacture due to its good strength and excellent stable corrosion property. The composition of the used Al-7075 alloy is shown in Table 1. The alloys in this series are classified into two types, Al-Zn-Mg-Cu alloys and Al-Zn-Mg alloys. The first type of alloys is the strongest of the aluminum alloys while the second one can be used in welded structures. The Al-Zn-Mg-Cu alloy is used as an ultra-super duralumin for aircraft materials, sporting goods, and other products. However, the Al-Zn-Mg alloy has a relatively high strength and it was primarily developed as welding structural material that can be thermally treated. In addition, the Al-Zn-Mg alloy can be used for structural and other materials in trains, including bullet trains. There are different types of aluminum 7075 alloy according to its temper like 7075-0 (un-heat treated), 7075-T6, 7075-T7, etc. It should be noted that the temper affects strongly on the alloy hardness properties such as elongation, tensile strength, and yield strength. In this study, an Al 7075-0 alloy is used which un-heat treated has the following hardness properties shown in Table 2.

The commercial alloy is cut into pieces with a dimension of 4 cm (radius) and 30 mm (thickness) by electric discharge machining (EDM) wire cutting. In this study, Sandblasting technique was used to clean the surface and to remove the rough spots using high pressure. After that the surface was further polished to a mirror state by using SiC paper (1000, 2400, 4000 grades). Finally, the surface was cleaned by ethanol or acetone.

2.2. Experimental setup

A nanosecond Nd:YAG laser (POWERLITE™ Precision II 8000, Continuum laser) is used in the experiment. The fundamental wavelength (1064 nm) is frequency doubled in BBO crystal (SHG) to 532 nm. Both laser beams are plane polarized after passing through a polarizer in the laser system. The full width at half maximum (FWHM) of the laser is fixed to 7 ns at a nominal wavelength of 1064 nm through Q-switch mode operation and repetition rate of 10 Hz. In addition, The laser energy (E) is varied from 0.1 to 0.9 J by tuning with a variable delay between oscillator and amplifier of the Nd:YAG laser. In addition, laser spot diameter

Table 2
Mechanical properties of Al-7075 alloy.

Mechanical property	Value
Density ($\times 1000$ kg/m^3)	2.8 at 25 °C
Poisson's Ratio	0.33 at 25 °C
Elastic Modulus (GPa)	70–80 at 25 °C
Tensile Strength (Mpa)	220
Yield Strength (Mpa)	95
Elongation (%)	17 at 25 °C
Hardness (HB500)	80 at 25 °C
Shear Strength (MPa)	150 at 25 °C
Fatigue Strength (MPa)	160 at 25 °C

at focusing d_{min} is adjusted by varying the distance between the lens and the sample by using the knife edge method (Handa et al., 2010; Plass et al., 1997). The experimental parameters such as laser energy (E_p), laser spot diameter (D) and laser number of pulses (N_p) of LPwC are listed in Table 3.

The LPwC process was carried by using a target samples placed on a holder place which was placed onto a moving stage. The moving stage rests on a computer controlled XY translation stage that can move in the X and Y directions during the peening process with an accuracy of ±5 μm as shown in schematic diagram in the Fig. 2. Next, a high power pulsed laser is focused onto the target material surface by using a lens (focal length = 7 cm).

The peak power density (G) are calculated by the following equations (Sano et al., 2006).

$$d_{min} = 2.44 \frac{f\lambda}{D} \tag{1}$$

$$A_p = \pi d_{min}^2 \tag{2}$$

$$G = \frac{E_p}{(A_p T)} \tag{3}$$

where f is the focal length (mm), λ is the wavelength (μm), D the laser spot diameter (mm), d_m, is the diameter of the central spot at focusing, A_p is the beam spot area at focusing, and T is the full width at half maximum (FWHM) of the laser pulse (7 ns in the current experiment). In the LPwC the incident laser pulse penetrates into the surface of the material within the penetration depth. This study of penetration depth was studied carefully by studying the effect of laser directly on the sample edge as shown in Fig. 3. To assess the hardness across the sample region, hardness measurements were taken using a micro-hardness machine (Shimaduz, micro-hardness tester, model: HMV-2E (344-04109-22), V ~ 100–120, 220–240, 50–60 Hz, 300 VA, Japan). The surface analysis was performed on the as-peened surface with scanning electron microscope (JXA-840A Electron Probe Micro analyzer JEOL-Japan Scanning Electron Microscope).

3. Results and discussions

3.1. Surface analysis and microstructure

Fig. 4 shows the image of the appearance of the aluminium alloy Al-7075 sample before and after LPwC process. It is evident from this Figure that the surface color changed from metallic to grayish at the instant of laser irradiation. This is caused by the

Table 1
Chemical compositions of Al-7075 alloy (wt%).

Al	Cr	Cu	Mg	Mn	Si	Ti	Zn	Fe	Other
87.1	0.28	2	2.1	<0.3	<0.4	<0.2	5.1	<0.2	<0.15

Table 3
Experimental Parameters of Laser Peening Without Coating (LPwC).

| Experimental parameters	Values
laser energy (E_p)	0.9 J
Focal length (f)	70 mm
Wavelength (μm)	1.064 μm, 0.532 μm
Laser spot diameter (D)	10 mm
Number of pulses (N_p)	300 pulses
FWHM (T)	7 ns
Diameter of the central spot at focusing (d_{min})	18.2 μm for λ = 1.064 μm
Beam spot area at focusing (A_P)	$259.5*10^{-12}$ m
Beam spot area at the used lens (A_L)	$78.6*10^{-6}$ m
Peak power density at focusing (G_P)	50 TW/cm^2
Peak power density at the used lens (G_L)	0.16 GW/cm^2
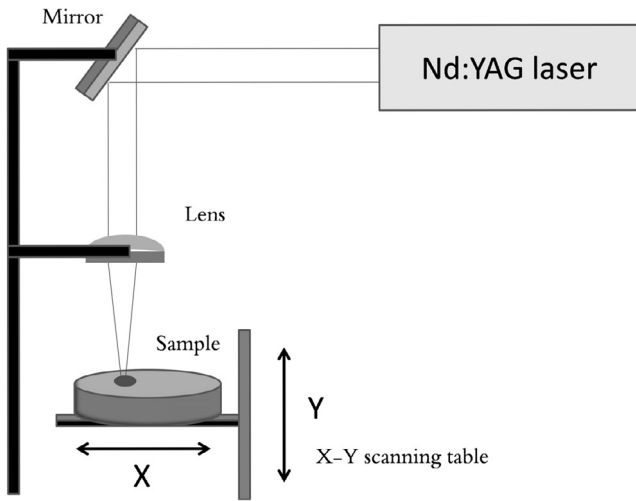
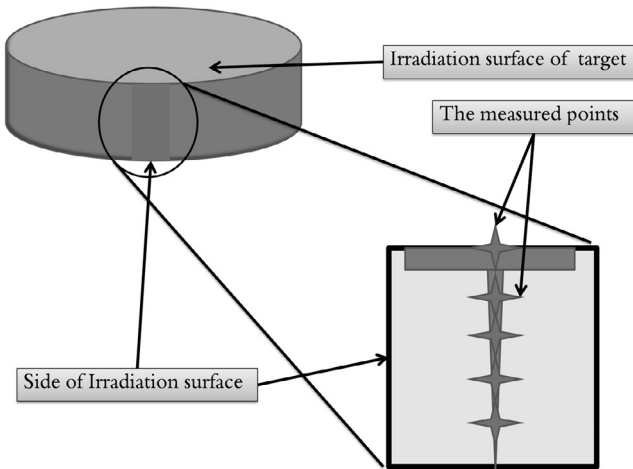**Fig. 2.** Schematic representation of the experiment setup.

Fig. 3. Schematic representation of Vickers micro hardness measurements.

Fig. 4. Schematic representation of the profile surface of the used Al alloy before and after the effect of the LPwC process.

Fig. 5. SEM micrograph image of an unpeened Al-alloy surface.

Fig. 6. SEM micrograph image of peened Al-alloy surface by 10pulses/mm2.

reaction of the surface with nascent-state oxygen supplied from active plasma and the intense electric field of the focused laser pulse (Sano et al., 2000).

The SEM micrograph images of the unpeened and peened surfaces are represented in Fig. 5:9. The polished unpeened surface appeared relatively smooth (Fig. 5), while the laser peened surface indicates large number of indentations (Fig. 6). The laser peened surface as compared to unpeened layer appears different due to the depressed layer caused by shock wave compression on LPwC surface. The solidified ablated products can be observed in the
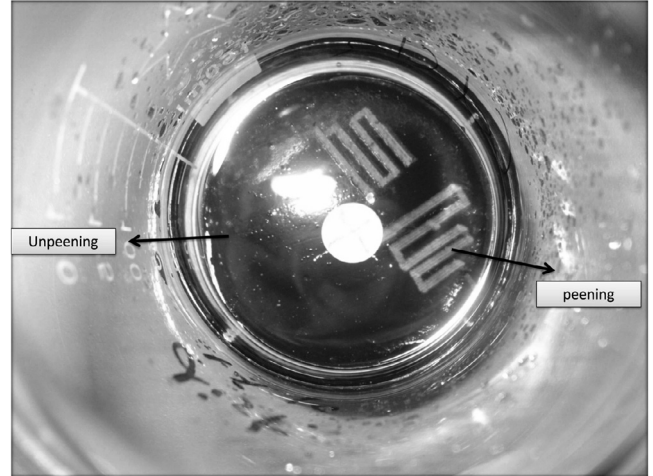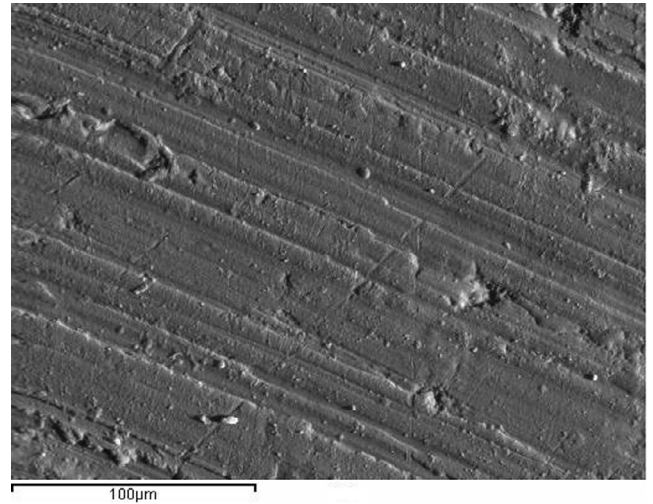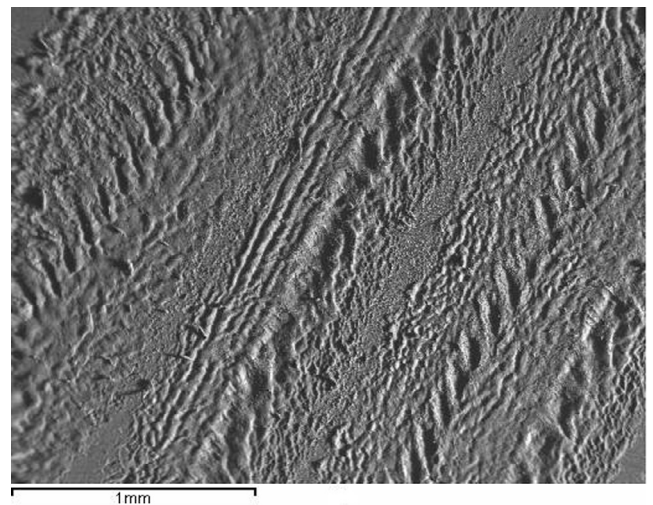
magnified images of the cross section is presented in Figs. 7–9. The polished unpeened surface of the cross section appeared relatively smooth (Fig. 7). The surface of peened Al-alloy by 10 pulse/mm^2 (Fig. 8) as compared to that peened Al-alloy by 100 pulse/mm^2 (Fig. 9) appeared different. This may be due to the increase of ablative interaction and thermal impact on the surfaces when the number of pulses increased. As the laser pulse density increased indentation becomes wider and deeper. It was previously reported that during LPwC there was a melting of the top surface layer (less than 1 mm deep from the surface) and there solidification of some of these ablative products leading to the development of micro-cracks to relax the stress during cooling (Maawad et al., 2012). This may be the effect of step by step peening along the Y-axis. However no micro-cracks were observed in the current SEM micrograph. These valleys induced due to ablative interaction and shock wave pressure on the surfaces can be observed on the top surface. The cross sectional observation confirms the absence of melted layer or micro-crack in the subsurface. This confirms that surface melting due to direct laser interaction does not have any appreciable effect beyond a depth of few micrometers from the top surface. The short laser pulse duration makes the LPwC process thermodynamically non-equilibrium which could be the reason for low thermal effect (or damage) even though the surface is not protected with any of the coating material (Sanchez, 2007; Sano et al., 2006, 1997).

3.2. Hardness properties

The hardness properties effects of the LPwC are evaluated based on micro-hardness analysis which can be calculated by using the Vickers hardness test (Sakharova et al., 2009). This test is often easier than other hardness tests since the required calculations are independent of the size of the indenter. In addition the indenter can be used for all materials irrespective of hardness. The basic principle of hardness measurements is to observe the questioned material's ability to resist plastic deformation from a standard source. The unit of hardness given by this test is known as the Vickers Pyramid Number (HV). In this study, for each depth point five measurements are taken and the average value is calculated. Standard deviations of the trials are included in the graph as an error bar. The Vickers micro-hardness measurement data of the aluminium alloy Al-7075 surface is summarized in Fig. 10:12.
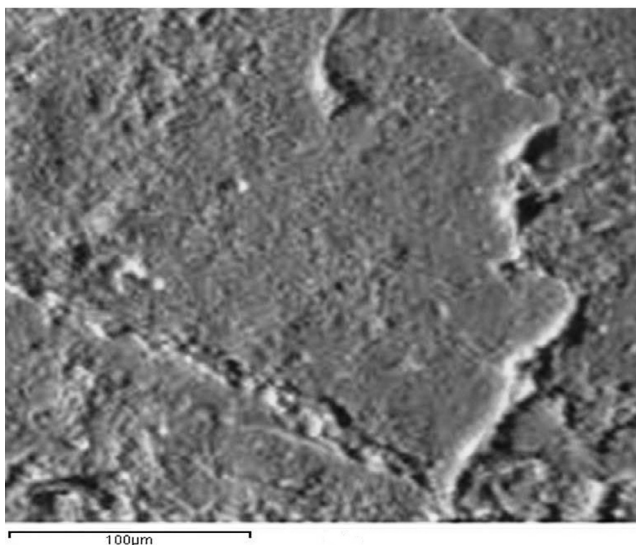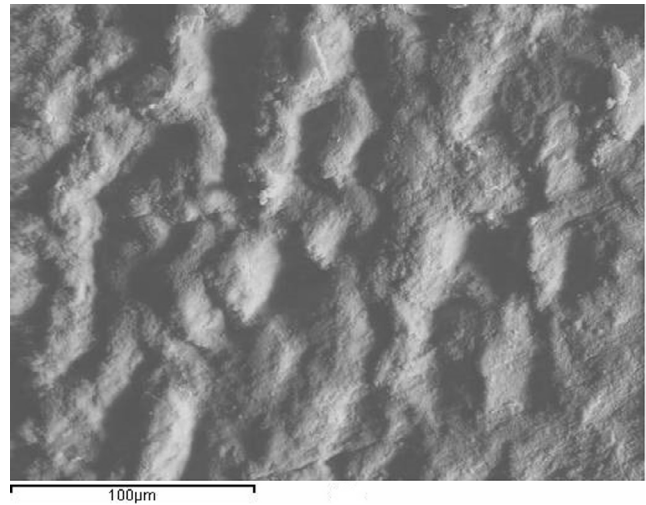

Fig. 8. SEM micrograph of magnified image of peened Al-alloy cross section surface by 10pulses/mm2.

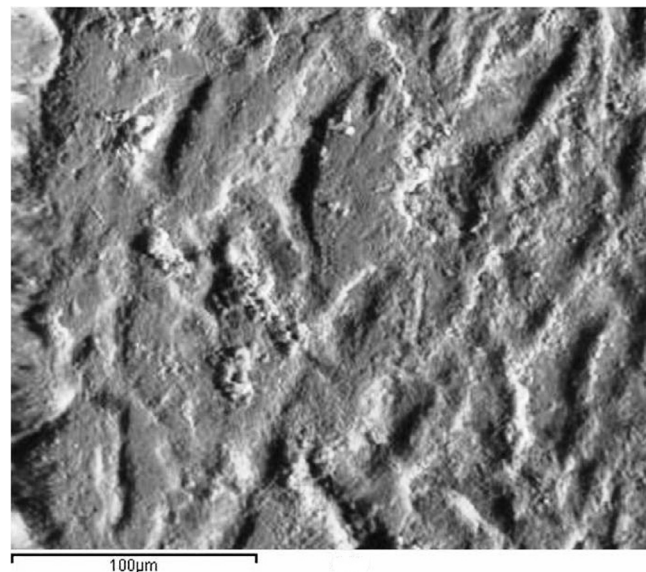**Fig. 9.** SEM micrograph of magnified image of peened Al-alloy cross section surface by 100pulse/mm2.

Fig. 7. SEM micrograph image of an unpeened Al-alloy cross section surface.

Fig. 10 shows the Vickers micro-hardness of the aluminium alloy Al-7075 surface as a function of the laser energy for nanosecond laser irradiation at infrared region (1064 nm) and visible region (532 nm). It can be observed that the hardness of the surface increases linearly with the laser energy in both cases of irradiation. However, the IR-irradiation (1064 nm) laser is slightly better at hardening. These changes of the hardness are due to the shock-waves that are generated by the expansion of high-pressure plasma caused by a pulsed laser. An intense laser pulse interacting with a solid target immediately causes the surface layer to instantaneously vaporize into a high-temperature and high-pressure plasma. The ablated plasma expands from the surface and, in turn, exerts a pressure on the face of the target, as a result compressive waves are induced in the solid target, and hence a shockwave is propagated through the sample. When the peak pressure created by the shockwave is above the dynamic yield stress, the metal is plastically deformed at the surface. This will induce a compressive residual stress in the surface of the part and thus increase the
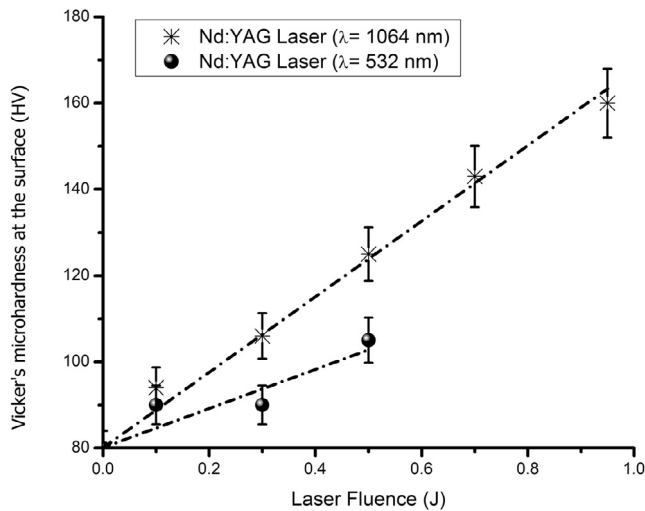
Fig. 10. Vickers micro hardness as a function of laser energy for nanosecond laser.

Fig. 12. Vickers micro hardness as a function of number of pulses.

resistance of the metal to surface-related failures such as fatigue, fretting fatigue, and stress corrosion cracking. Therefore, the plasma formation and the shockwave are increased by increasing the laser intensity (Fan et al., 2005). Fig. 11 shows Vickers microhardness of peened and unpeened material as a function of surface depth. The cross-section of the specimen along the Y axis has been taken for the investigation. Measurements were made with 50 g load and 10 s hold time. For each depth value, five measurements were taken and the average was represented. In this experiment, the laser energy is adjusted to be 0.5 J at infrared region (1064 nm) and visible region (532 nm). The dashed line in this figure indicates the normal hardness before laser irradiation. From this figure, it's clear that the measured micro-hardness is decreased by increasing the depth from the surface of the sample. This is due to the specimen heating characteristic during the LSP process which produces shockwave under the effect of plasma confinement (Rutkevich et al., 1997). The shockwave propagates in an aluminium alloy and decreases in amplitude as the energy of the shock is spread over greater areas (Lake and Todd, 1961). After the shock radius has become about one-fifth greater than its initial value, the density and internal energy are discontinuous leading to destroy the radial symmetry of the flow (Sobek and Todd, 1962). In
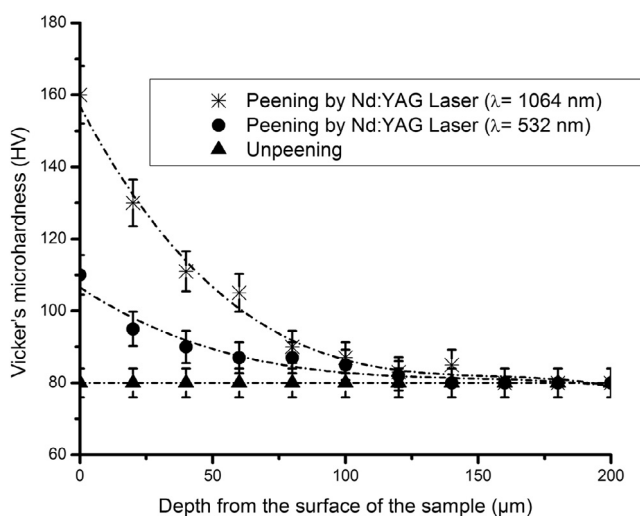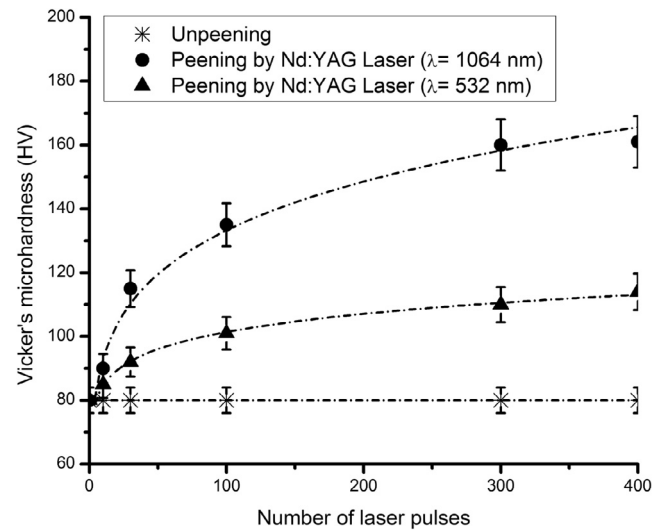
addition, there are differences in behaviour at infrared region (1064 nm) and at visible region (532 nm) measurements versus increasing the depth from the surface of the sample. That is because the infrared absorption is just heating of the surface since it increases molecular vibrational activity. However, the infrared is less strongly than visible light in energy. So, the infrared radiation does penetrate the surface and produced shockwaves further than visible light. So, the effect of hardness in case of infrared is higher than that if visible. Fig. 12 shows Vickers micro-hardness as a function of number of pulses. From this Figure, it is clear that the micro-hardness of materials increases as the number of pulses increases. Furthermore, the magnitude of the micro-hardness resulted from Nd:YAG (1064 nm) is larger than that from Nd:YAG (532 nm). However, in case of unpeening, the hardness of the material remains without any change. The increase of the magnitude of the micro-hardness is due to the effect of the high intensities of the laser ablation by fast laser, type of pulsed laser contains nanosecond laser and microsecond laser, which leads to heat conduction, melting, evaporation, and plasma formation. Then, the shockwave is produced and the hardness is increased. Therefore, the time of ablation and plasma formation are increased by increasing the number of shots. However, when the number of shots is increased more than 300 shots, the plasma is finished and the saturation occurs because the nanosecond ablation process is still dominated by classical beam-matter interaction based on melting, evaporation and plasma formation. Yet, from the beginning evaporation and melt expulsion occurred leading to a significant material removal. With increasing pulse number the diameter of the ablation zone increases. With increasing depth of the drill hole the expulsion of melt becomes less efficient (Leitz et al., 2011). Therefore, the hardness can't be further increased and saturation occurs.

4. Conclusion

In summary, LSP specially without coating (LPwC) is successfully performed on Al-7075 alloy using Nd:YAG laser to investigate the feasibility of nanosecond laser shock peening by using the fundamental wavelength (1064 nm) and its second harmonic (532 nm). It is found that the surface hardness of the Al-7075 alloy increased linearly with the increase in the laser energy and number of laser shots irradiated per unit area. Besides, the hardness value of the laser peened specimen offers a maximum improvement of

Fig. 11. Vickers micro hardness as a function of depth for nanosecond laser.

80HV near to the surface which represents the double increasing of the hardness by using the LPwC technique. This investigation gives a great potential solution to increase the durability of engineering components and decrease their sensitivity to foreign object damage (FOD).

References

Bajat, J.B. et al., 2010. Corrosion protection of aluminium pretreated by vinyltriethoxysilane in sodium chloride solution. Corros. Sci. 52 (3), 1060–1069.

Barcikowski, Stephan, Menéndez-Manjón, Ana, Chichkov, Boris, Brikas, Marijus, Račiukaitis, Gediminas, 2007. Generation of nanoparticle colloids by picosecond and femtosecond laser ablations in liquid flow. Appl. Phys. Lett. 91 (8), 083113.

Barmina, E.B., Stratakis, E., Fotakis, C., Shafeev, G.A., 2010. Generation of nanostructures on metals by laser ablation in liquids new results. Quantum Electron. 40 (11).

Besner, S., Degorce, J.-Y., Kabashin, A.V., Meunier, M., 2005. Influence of ambient medium on femtosecond laser processing of silicon. App. Surf. Sci. 247, 163–168.

Brus, L.E., 1984. Electron–electron and electron-hole interactions in small semiconductor crystallites: the size dependence of the lowest excited electronic state. J. Chem. Phys. 80, 4403.

Cauble, R. et al., 1993. Demonstration of 0.75 Gbar planar shocks in x-ray driven colliding foils. Phys. Rev. Lett. 70 (14), 2102–2105.

Darwish, A.M. et al., 2015. Synthesis of nano-cadmium sulfide by pulsed laser ablation in liquid environment. Spectrosc. Lett. 48 (9), 638–645.

Darwish, A.M. et al., 2016. Investigation of factors affecting the synthesis of nano-cadmium sulfide by pulsed laser ablation in liquid environment. Spectrochim. Acta Part A Mol. Biomol. Spectrosc. 153, 315–320.

Ding, K., Ye, L., 2006a. Laser shoReferences Shock Peening. CRC Press WP. Chapters 1 and 2.

Ding, K., Ye, L., 2006b. Laser Shock Peening: Performance and Process Simulation. Woodhead Publishing, Cambridge.

Ezuber, H., El-Houd, A., El-Shawesh, F., 2008. A study on the corrosion behavior of aluminum alloys in seawater. Mater. Des. 29 (4), 801–805.

Fabbro, R. et al., 1990. Physical study of laser-produced plasma in confined geometry. J. Appl. Phys. 68 (2), 775–784.

Fairand, B.P., Clauer, A.H., 1976. Effect of water and paint coatings on the magnitude of laser-generated shocks. Opt. Commun. 18 (4), 588–591.

Fairand, B.P. et al., 1972. Laser shock-induced microstructural and mechanical property changes in 7075 aluminum. J. Appl. Phys. 43 (9), 3893–3895.

Fairand, B.P. et al., 1974. Quantitative assessment of laser-induced stress waves generated at confined surfaces. Appl. Phys. Lett. 25 (8), 431–433.

Fan, Y. et al., 2005. Wave-solid interactions in laser-shock-induced deformation processes. J. Appl. Phys. 98 (10), 104904–104911.

Gomez-Rosas, G. et al., 2010. Laser Shock Processing of 6061-T6 Al alloy with 1064 nm and 532 nm wavelengths. Appl. Surf. Sci. 256 (20), 5828–5831.

Graham, R.A., Yang, L.C., 1975. Inherent time delay for dielectric breakdown in shock-loaded x-cut quartz. J. Appl. Phys. 46 (12), 5300–5301.

Handa, S. et al., 2010. Extended knife-edge method for characterizing sub-10-nm X-ray beams. Nucl. Instrum. Methods Phys. Res., Sect. A 616 (2–3), 246–250.

Harada, Y., Fukaura, K., Haga, S., 2007. Influence of microshot peening on surface layer characteristics of structural steel. J. Mater. Process. Technol. 191 (1–3), 297–301.

Hu, Y., Yao, Z., 2008. Overlapping rate effect on laser shock processing of 1045 steel by small spots with Nd:YAG pulsed laser. Surface Coatings Technol. 202, 1517–1525.

Kazakevich, P.V., Simakin, A.V., Voronov, V.V., Shafeev, G.A., 2006. Laser induced synthesis of nanoparticles in liquids. Appl. Surf. Sci. 252, 4373–4380.

Lake, H.R., Todd, F.C., 1961. Digital Computer Solution for the Propagation of a Spherical Shock Wave in Aluminum. In: PROC. OF THE OKLA. ACAD. OF SCI.

Leitz, K.-H. et al., 2011. Metal ablation with short and ultrashort laser pulses. Phys. Procedia 12 (Part B), 230–238.

Maawad, E. et al., 2012. Investigation of laser shock peening effects on residual stress state and fatigue performance of titanium alloys. Mater. Sci. Eng., A 536, 82–91.

Masaki, K. et al., 2007. Effects of laser peening treatment on high cycle fatigue properties of degassing-processed cast aluminum alloy. Mater. Sci. Eng., A 468–470, 171–175.

Montross, C.S., Florea, V., 2001. The influence of coatings on subsurface mechanical properties of laser peened 2011-T3 aluminum. J. Mater. Sci. 36, 1801–1807.

Montross, C.S. et al., 2002. Laser shock processing and its effects on microstructure and properties of metal alloys: a review. Int. J. Fatigue 24 (10), 1021–1036.

Mutombo, K., Toit, M.D., 2011. Corrosion fatigue behaviour of aluminium alloy 6061-T651 welded using fully automatic gas metal arc welding and ER5183 filler alloy. Int. J. Fatigue 33 (12), 1539–1547.

O'Regan, B., Grätzel, M., 1991. A low-cost, high-efficiency solar cell based on dye-sensitized colloidal TiO$_2$ films. Nature 353, 737–740.

Ochi, Y. et al., 2010. Effects of laser peening treatment without protective coating on axial fatigue property of aluminum alloy. Procedia Eng. 2 (1), 491–498.

Odhiambo, D., Soyama, H., 2003. Cavitation shotless peening for improvement of fatigue strength of carbonized steel. Int. J. Fatigue 25 (9–11), 1217–1222.

Oguri, K., 2011. Fatigue life enhancement of aluminum alloy for aircraft by Fine Particle Shot Peening (FPSP). J. Mater. Process. Technol. 211 (8), 1395–1399.

Panagopoulos, C.N., Georgiou, E.P., Gavras, A.G., 2009. Corrosion and wear of 6082 aluminum alloy. Tribol. Int. 42 (6), 886–889.

Peyre, P. et al., 1996. Laser shock processing of aluminium alloys. application to high cycle fatigue behaviour. Mater. Sci. Eng., A 210 (1–2), 102–113.

Peyre, P. et al., 2000. Surface modifications induced in 316L steel by laser peening and shot-peening. Influence on pitting corrosion resistance. Mater. Sci. Eng., A 280 (2), 294–302.

Plass, W. et al., 1997. High-resolution knife-edge laser beam profiling. Opt. Commun. 134 (1–6), 21–24.

Rodopoulos, C.A. et al., 2003. Effect of controlled shot peening and laser shock peening on the fatigue performance of 2024-T351 aluminum alloy. J. Mater. Eng. Perform. 12 (4), 414–419.

Romain, E. et al., 2013. Observation of the shock wave propagation induced by a high-power laser irradiation into an epoxy material. J. Phys. D Appl. Phys. 46 (23), 235501.

Rubio-González, C. et al., 2004. Effect of laser shock processing on fatigue crack growth and fracture toughness of 6061-T6 aluminum alloy. Mater. Sci. Eng., A 386 (1–2), 291–295.

Rubio-González, C. et al., 2011. Effect of laser shock processing on fatigue crack growth of duplex stainless steel. Mater. Sci. Eng., A 528 (3), 914–919.

Rutkevich, I., Zaretsky, E., Mond, M., 1997. Thermodynamic properties and stability of shock waves in metals. J. Appl. Phys. 81 (11), 7228–7241.

Sakharova, N.A. et al., 2009. Comparison between Berkovich, Vickers and conical indentation tests: a three-dimensional numerical simulation study. Int. J. Solids Struct. 46 (5), 1095–1104.

Sanchez, D.B., 2007. The Surface Plasmon Resonance of Supported Noble Metal Nanoparticles: Characterization, Laser Tailoring, and SERS Application. Madrid University (PhD thesis).

Sano, Y. et al., 1997. Residual stress improvement in metal surface by underwater laser irradiation. Nucl. Instrum. Methods Phys. Res., Sect. B 121 (1–4), 432–436.

Sano, Y. et al., 2000. Process and application of shock compression by nano-second pulses of frequency-doubled Nd:YAG laser. Proc. SPIE High-Power Lasers Manuf. 3888, 294–306.

Sano, Y., Obata, M., Kubo, T., Mukai, N., Yoda, M., Masaki, K., et al., 2006. Retardation of crack initiation and growth in austenitic stainless steels by laser peening without protective coating. Mater. Sci. Eng. A 334, 334–340.

Sano, Y. et al., 2006. Retardation of crack initiation and growth in austenitic stainless steels by laser peening without protective coating. Mater. Sci. Eng., A 417 (1–2), 334–340.

Sathyajith, S., Kalainathan, S., 2012. Effect of laser shot peening on precipitation hardened aluminum alloy 6061–T6 using low energy laser. Opt. Lasers Eng. 50 (3), 345–348.

Sathyajith, S., Kalainathan, S., Swaroop, S., 2013. Laser peening without coating on aluminum alloy Al-6061-T6 using low energy Nd:YAG laser. Opt. Laser Technol. 45, 389–394.

Smolej, A., Skaza, B., Markoli, B., Klobčar, D., Dragojević, V., Slaček, E., 2012. Superplastic behaviour of AA5083 aluminum alloy with scandium and zirconium. Mater. Sci. Forum 706 (709), 395–401.

Sobek, B.A., Todd, F.O., 1962. Penetration of an Initially Radial Shock Wave Through an Aluminum-Glass Interfacel. PROC. OF THE OKLA. ACAD. OF SCI.

Trdan, U., Ocaña, J.L., Grum, J., 2010. Surface modification of aluminium alloys with laser shock processing. J. Mech. Eng. 57 (5), 385–393.

Trdan, U. et al., 2012. Laser shock peening without absorbent coating (LSPwC) effect on 3D surface topography and mechanical properties of 6082-T651 Al alloy. Surf. Coat. Technol. 208, 109–116.

Trueba, M., Trasatti, S.P., 2010. Study of Al alloy corrosion in neutral NaCl by the pitting scan technique. Mater. Chem. Phys. 121 (3), 523–533.

Vargel, C., 2004. Corrosion of Aluminum. Elsevier Science, San Diego, USA.

Vázquez, J., Navarro, C., Domínguez, J., 2012. Experimental results in fretting fatigue with shot and laser peened Al 7075-T651 specimens. Int. J. Fatigue 40, 143–153.

Warren, A.W., Guo, Y.B., Chen, S.C., 2008. Massive parallel laser shock peening: simulation, analysis, and validation. Int. J. Fatigue 30 (1), 188–197.

White, R.M., 1963. Elastic wave generation by electron bombardment or electromagnetic wave absorption. J. Appl. Phys. 34 (7), 2123–2124.

Yang, J.M. et al., 2001. Laser shock peening on fatigue behavior of 2024-T3 Al alloy with fastener holes and stopholes. Mater. Sci. Eng., A 298 (1–2), 296–299.

Yue, T.M., Yan, L.J., Chan, C.P., 2006. Stress corrosion cracking behavior of Nd:YAG laser-treated aluminum alloy 7075. Appl. Surf. Sci. 252 (14), 5026–5034.

Yuji Sano, M.O., Kubo, Tatsuya, Mukai, Naruhiko, Yoda, Masaki, Masaki, Kiyotaka, Ochi, Yasuo, 2006. Retardation of crack initiation and growth in austenitic stainless steels by laser peening without protective coating. Mater. Sci. Eng. A 417 (1–2), 334–340.

Zeldovich, Y., Raizer, Y., 1967. Physics of Shock Waves and High Temperature Hydrodynamic Phenomena. Academic Press.

Zhang, X.C. et al., 2010. Improvement of fatigue life of Ti–6Al–4V alloy by laser shock peening. Mater. Sci. Eng., A 527 (15), 3411–3415.

Zhou, J.Z. et al., 2012. Effect of repeated impacts on mechanical properties and fatigue fracture morphologies of 6061-T6 aluminum subject to laser peening. Mater. Sci. Eng., A 539, 360–368.